

# Performance-Based Seismic Assessment of a Recently Built High-Speed Rail Viaduct in Spain. The Archidona Viaduct

Carlos Gordo-Monso<sup>1</sup>, Eduardo Miranda<sup>2</sup>

## ABSTRACT

High-Speed Rail Lines (HSRL) have experienced in recent years an unprecedented development and expansion in Southern Europe. In particular, Spain has nearly 1,800 miles (2,880 km) HSRL, with a significant portion of these in regions of moderate seismic hazard. The Archidona Viaduct, a recently erected composite steel-concrete viaduct in the new Cordoba-Granada HSRL, is a 1.97 miles (3,150 m) long viaduct built without intermediate expansion joints and is located in a site with an expected peak ground acceleration (PGA) of 0.14-g for a return period of 500 yr. The viaduct has 62 framed piers (bents) which laterally restrain transverse displacement but allow for longitudinal displacement through spherical sliding bearings. The longitudinal displacement is restrained at a single stiff pier, located roughly in the middle of the viaduct. This paper presents the results of a series of static and dynamic analyses of a typical 66 ft (20 m) high framed pier and its corresponding foundation, conducted in order to assess its seismic performance. In particular, to assess the seismic collapse capacity, and to identify different characteristic features on the seismic behavior of the Archidona Viaduct at increasing levels of seismic intensity. A special emphasis is placed on the estimation of train derailment due to seismically induced rail deformations.

## INTRODUCTION

The Archidona Viaduct is located in the High-Speed Rail Line connecting the southern Spain cities of Cordoba and Granada. The viaduct is conceived in the purpose of crossing a 1.97 miles (3,150 m) long valley meeting certainly special conditions (Millanes-Mato et al. 2011):

- The viaduct is located in a moderately hazardous seismic site (500 year  $PGA=0.14\cdot g$ ).
- The mean pier height is approximately 66 ft (20 m).
- The request of the track owner to avoid, as much as possible, the use of rail expansion joint devices to limit the associated maintenance costs, but complying with the maximum displacement limits allowed by current state-of-the-art rail expansion devices 47¼ in (1200mm) (Hess, 2009).

The solution of several simply supported spans, which in general is suitable for great length and low height viaducts, was discarded due to the longitudinal flexibility of the substructure (set of piers and pile foundation), which yielded excessive track displacements under the train braking and service-level earthquake ground motions. Moreover, this solution was overly penalized regarding the design earthquake situation. Given that it was not advisable to place rail expansion joint devices within the deck, only two of them were placed at the abutments, and the deck's fixed point was placed roughly in the viaduct center, allowing a total maximum dilation

---

1 Graduate Student, Stanford University and Design Engineer, IDEAM, Velazquez 41, 1-A, 28005 Madrid, Spain  
2 Assoc. Prof., Stanford University, 473 Via Ortega, Room 281, Stanford, CA 94305

length around 1 mile (1,600 m) (Figure 1 and Figure 4). A prestressed concrete deck solution for this dilation length would have yielded longitudinal displacements, due to thermal and hygrometric actions, larger than those allowed by current state-of-the-art rail expansion joint devices. Therefore, a composite steel-concrete deck solution was chosen in order to mitigate the effects of shrinkage and creep.

The span length distribution of the viaduct is 114ft+30x164ft+114ft (35m+30x50m+35m). The 164 ft (50 m) standard span length was chosen on the basis of the pier height, and in order to achieve both weight and dimensions suitable for erection by crane rising (Figure 2). The retained solution for the deck consists of a constant depth composite steel-concrete cross section, formed up by two steel welded I-beams 9 ft 8 in (2.95 m) deep, and an upper reinforced concrete slab 15¾ in (0.40 m) thick linking both steel beams, which are 19 ft 8 in (6 m) apart. A bottom reinforced concrete slab acts as a compression member within the hogging zone (double composite action), and closing the torsion circuit within the sagging zone.

Given that the central pier is considered as the only fixed point in the longitudinal direction of the viaduct, it was designed as a triangular shape frame, in order to provide a stiff truss mechanism to limit displacements due to braking forces (Figure 4). On the other hand, the other (typical) piers are designed to allow for the longitudinal movement of the deck through the use of spherical sliding bearings with a top flat PTFE surface, and to restrain transverse displacement through a central shear key. The shear key is built of concrete on the pier side, and as a steel protrusion of the diaphragm on the deck side, sandwiching twin PTFE sliding devices.

## OBJECTIVE OF THE STUDY

High-Speed Rail Lines (HSRL) structures differ from highway bridges in the sense that they must meet different often more strict service conditions, in addition to structural requirements, to ensure the safety of rail traffic. Aspects that in highway bridges can be considered as serviceability conditions, like vertical or transverse deformability, are of the utmost importance in HSRL viaducts, given that the safety of the traffic depends largely on the track geometry (Nasarre, 2009). It is so much so, that an horizontal misalignment as small as ¾ in (20 mm) can force a reduction of the train's speed at the damaged section of the track, and a misalignment of 3 in (80 mm) can drive to the closure of the track for alignment repair (Pitilakis et al., 2011).



Figure 1. General view of the Archidona Viaduct.



Figure 2. Deck assembly and crane erection.

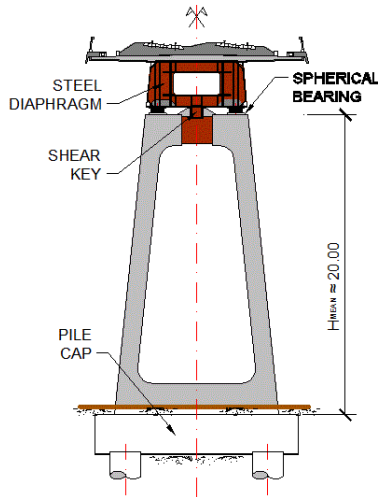


Figure 3. View of a typical pier (transv. fixed)



Figure 4. View of the central pier (longit. fixed point)

Although various studies have dealt with the expected performances, and the associated economic losses, of newer and older building structures under different earthquake intensities, much less work has been devoted to the expected seismic performance of bridge structures, especially in the low intensity range and for elements different than structural members. For instance, the European specifications (EN-1998-2) state that the performance of a bridge subjected to a low level intensity earthquake (high probability of occurrence) “*may cause only minor damage to secondary components and to those parts of the bridge intended to contribute to energy dissipation. All other parts of the bridge should remain undamaged*”, leaving unanswered the question of what the expected performance should be for the non-structural elements like the track, in the case of a HSRL viaduct. The Spanish specifications for earthquake design of bridges (NCSP-07) state that “*the frequent seismic action shall only cause minor damage to the bridge, and it will not be neither necessary to repair it immediately, nor to reduce the traffic after such an earthquake*”. Given that most of the previous work on the subject of post earthquake traffic capacity is related with the structural capacity of bridge piers after a seismic event (Terzic and Stojadinovic, 2010), there are not many references to which the engineers can refer to evaluate the relative importance of the frequent earthquake respective to the overall design.

In this regard, the objective of the study presented in this paper is to analyze the seismic behavior of a bridge designed according to the current European standards (EN-1998-1 and EN-1998-2), with the purpose of understanding how different design assumptions influence the expected performance of both the viaduct as a structure, and of the track which is a critical components for the functionality of the structure. In order to do so, the transverse behavior of a typical pier of the Archidona viaduct has been analyzed under seismic excitations of different intensities, following the PEER Performance-Based Earthquake Engineering methodology (Krawinkler and Miranda, 2004). Different mechanical characteristics of the set pier-foundation were studied. In particular, the following modeling assumptions that were analyzed are summarized in this work:

- Model 2: Analysis of the transverse behavior under the assumption of cracked stiffness, considered as a function of the Moment-Curvature diagram of the pier cross section (Priestley et al., 1996), and considering the foundation as infinitely stiff.

- Model 4: Analysis of the transverse behavior under the previous cracked condition, taking into account the decrease in stiffness due to the rocking behavior of the deep foundation.
- Model 6: Analysis of the transverse behavior under the assumption of cracked stiffness, considering the stiffness reduction due to both the strain penetration effect and shear cracking (Fardis, 2003).
- Model 8: Analysis of the transverse behavior under the previous cracked condition, taking into account the decrease in stiffness due to the rocking behavior of the deep foundation.

For the previously stated modeling assumptions, several Damage Measures (DM) related to different Engineering Demand Parameters (EDP) have been considered:

- Structural Damage Measures as DMs1: Yielding of the longitudinal reinforcement on the tension side. DSs2: Cover concrete spalling on the compression side. DSs3: Buckling of the longitudinal reinforcement on the compression side. These structural DM have been related to the maximum Column Drift Ratio as EDP, taking the perspective of several authors (Kunnath et al., 2006), (Mackie, 2003), (Mander, 2007).
- Collapse Damage Measures as DMc: The pier is assumed to collapse when the column drift ratio exceeds the value of IDR=10%, value for which the monotonic pushover analysis yields a zero base-shear value.
- Track Damage Measures as DMt1: Lateral track displacement corresponding to an immediate action on the railway traffic to ensure running safety (i.e. speed reduction until track repair). DMt2: Lateral track displacement corresponding to the closure of the track to ensure running traffic (Moderate track repair). DMt3: Lateral track displacement corresponding to the closure of the track (Extensive track repair). These track DM have been related to the Residual Column Drift Ratio, as a measure of the track misalignment/offset after an earthquake (Pitilakis et al., 2011).
- Safety Run Damage State as DSdr: Motion of the deck during an earthquake driving to the derailment of the train. This DM has been related to the Spectral Index as EDP (Luo, 2005), (Luo and Miyamoto, 2007).

## STRUCTURAL BEHAVIOR MODELLING

For the modelling of the bent structure the characteristic properties of the involved materials were considered, namely  $f'_c=5$  ksi (35MPa) for concrete members and  $f_y=75$  ksi (500MPa) for the steel reinforcement. The Mander model (Mander, 1988) was used to represent the concrete behavior both at the confined core and at the unconfined cover (Figure 6), and a bilinear stress-strain class C relationship (EN-1992-1) with an ultimate-to-yield stress ratio  $f_u/f_y=1.15$  has been used for the B500C reinforcement steel. The moment-curvature diagram of the top and bottom cross-sections of the columns has been evaluated at increasing axial load ratios (Figure 5) to obtain the cracked stiffness. It has been found that, due to the large steel ratio in the cross section, the cracked stiffness does not show a big dependence on the axial force, and an average value of  $I_{eff}=0.8 \cdot I_g$  (cracked inertia as a fraction of the gross inertia) has been considered adequate for the  $N/A_c \cdot f'_c=0.1$  ratio expected to act in the most loaded column.

The bent was modeled in OpenSees (OpenSees, 2004) as an elastic structure with concentrated plastic hinges at the base and top cross-sections. A strength and stiffness deterioration behavior (Ibarra et al, 2005) was considered for the concentrated hinges (Figure 8). It is known that the stiffness derived from the  $M-\phi$  relationship at the section level is not enough

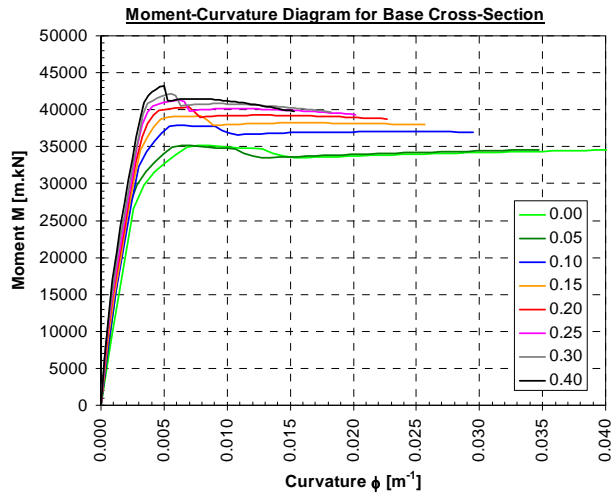


Figure 5. Moment-Curvature diagrams for axial load ratios ranging from  $N/A_c \cdot f_c' = 0.1$  to 0.4

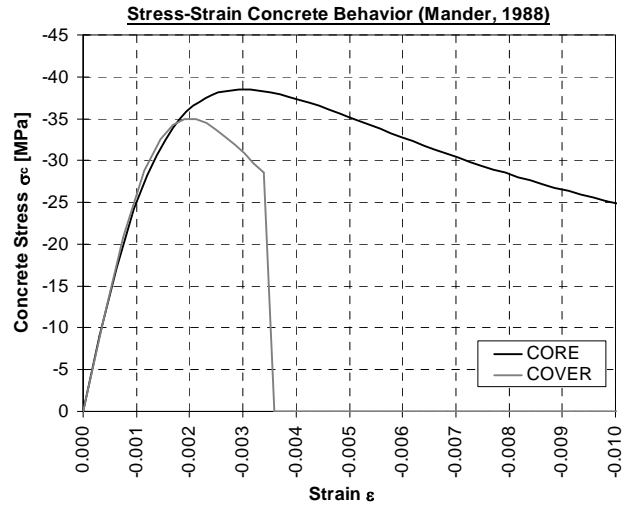


Figure 6. Concrete behavior at core and cover fibers (Mander, 1988)

to assess the total stiffness of the flexural members at high levels of load (Hasselton and Deierlein, 2007). The strain penetration (or bar slippage), and shear cracking mechanisms reduce the stiffness of the flexural member, and hence change the structural behavior of the bent. The stiffness expression proposed by Fardis (Fardis, 2009) was used to assess a cracked stiffness  $I_{eff} = 0.3 \cdot I_g$ . Two alternative assumptions were considered to account for stiffness variability by considering cracked stiffness as 80% and as 30% of the gross stiffness. Monotonic pushover analyses (Figure 7) were performed to assess the relative importance of the aforementioned parameters.

Another source of flexibility that was considered was the reduction in lateral and rotational stiffness at the base of the structure due to soil-structure interaction. As recognized by several authors (Kunnath et al., 2006), the behavior of the foundation can play a significant role in the assessment of the seismic performance of the viaduct. In this regard, two scenarios were analyzed: one with an infinitely stiff foundation, and another with a flexible foundation whose

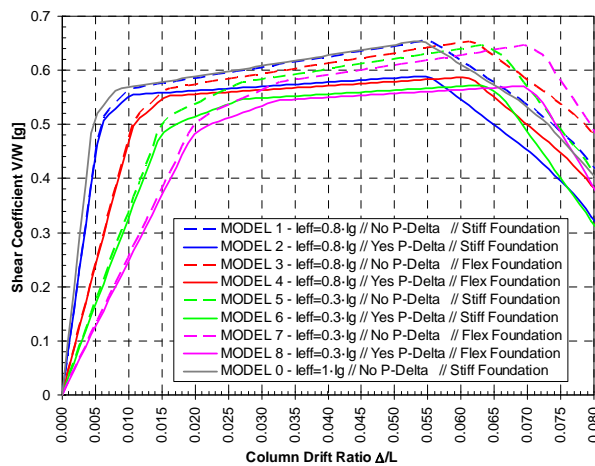


Figure 7. Monotonic pushover curves for different behavior models

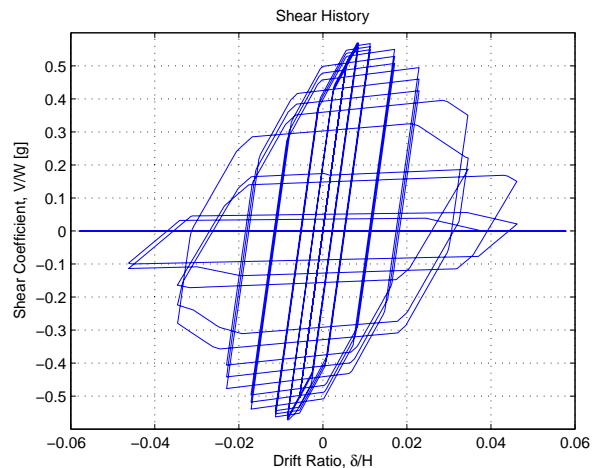


Figure 8. Cyclic pushover for model 2 behavior ( $I_{eff} = 0.8 \cdot I_g$ , Stiff foundation)



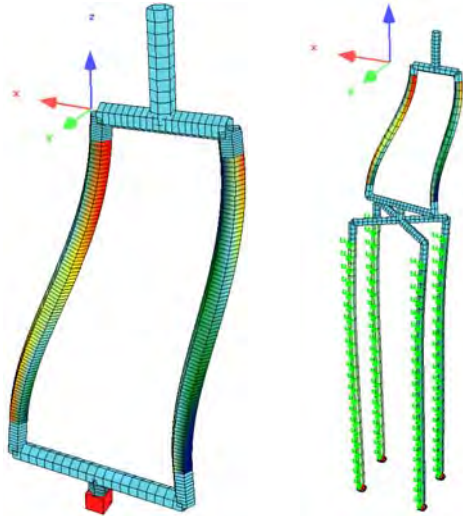


Figure 9. Fundamental modes for both the stiff foundation and flexible foundation models.

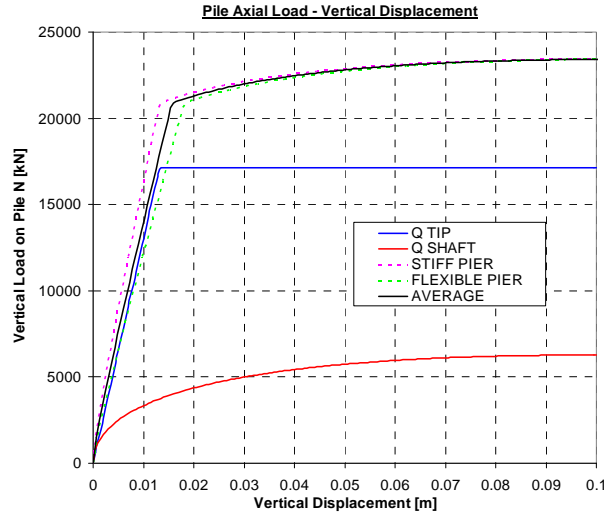


Figure 10. Equivalent pile axial stiffness, considering skin strength, tip strength, and concrete deformability.

equivalent parameters were derived from geotechnical data of the project (PoLam et al., 1998), (Mosher and Dawkins, 2000). The foundation is formed by 4 piles 5 ft (1.5 m) wide in diameter, tip supported on a firm but soft marl bedrock, characteristic of the Andalusian region, near 100 ft (30 m) deep below grade. The rock is therefore relatively stiff, but the piles are long enough to provide some degree of extra flexibility at the pile cap level. Furthermore, the clay soil between grade and bedrock allows for some shear-like lateral pile displacement. The periods of vibration in the transverse direction of the 4 models are summarized in TABLE I.

## SEISMIC HAZARD EVALUATION

The spectral acceleration at the characteristic period of each model was used as the Intensity Measure (IM) for characterizing the earthquake ground motion intensity.. The evaluation of the seismic hazard at the viaduct site has been performed according to the approximate hazard estimation provided by the Spanish Seismic Code (NCSP-07) (Figure 11), which has been corroborated by regional probabilistic hazard assessments (Benito et al., 2010).

## SEISMIC DEMAND (EDP) AND DAMAGE (DM) ESTIMATION

Force and deformation demands in the structure were computed at increasing levels of earthquake intensity by using Incremental Dynamic Analyses (IDA) (Vamvatsikos and Cornell, 2002), using ground motion scaled to match spectral acceleration at the different characteristic

TABLE I. CHARACTERISTIC PERIODS FOR BEHAVIOR MODELS

Model #	Assumed Behavior	Characteristic Period T
2	$I_{\text{eff}}=0.8 \cdot I_g$   Stiff Foundation	0.72 s
4	$I_{\text{eff}}=0.8 \cdot I_g$   Flexible Foundation	0.97 s
6	$I_{\text{eff}}=0.3 \cdot I_g$   Stiff Foundation	1.14 s
8	$I_{\text{eff}}=0.3 \cdot I_g$   Flexible Foundation	1.31 s

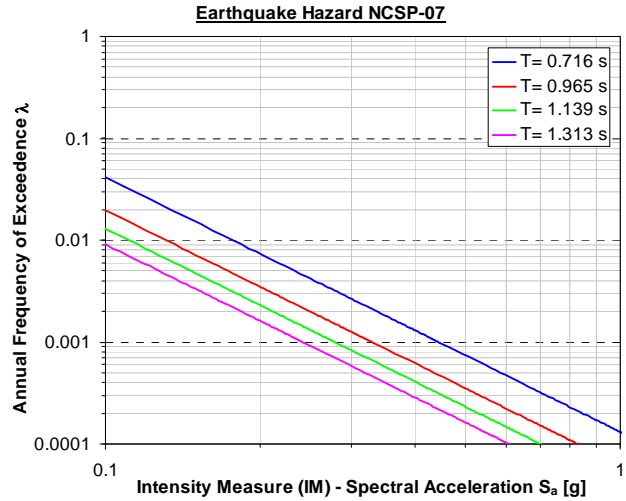


Figure 11. Earthquake Hazard at different fundamental oscillation periods

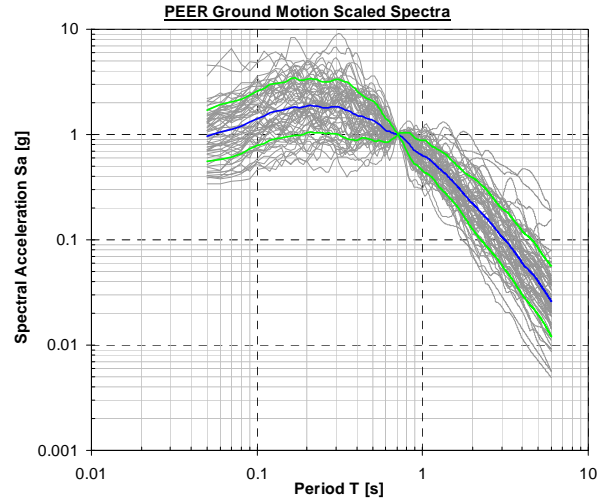


Figure 12. Ground motion set scaled to  $1 \cdot g$  at  $T=0.72s$ . Median in blue,  $\pm 1 \cdot \sigma$  in green.

periods for each different structural model (stiffness at the yielding of the first hinge) as illustrated in Figure 12. The set of ground motions was selected from the PEER ground motion database by using their online tool for ground motion selection (PEER, 2012). Sixty different ground motions were selected to match the design spectrum of the Spanish Seismic Code (NCSP-07).

As previously stated, the intended damage estimation is both for structural components and for some key nonstructural components critical to the functionality of the viaduct, namely the rail. For assessing structural damage, the EDP considered was the maximum column drift ratio, whereas for rail damage the EDP considered was the residual column drift ratio. This double approach is intended to measure the relative importance of both structural and nonstructural elements in the seismic assessment of the viaduct. Structural damage measure (DM) considered were those corresponding to the damage states of yielding in the longitudinal reinforcement (DMs1), compression concrete spalling (DMs2), and buckling of the longitudinal compression reinforcement (DMs3), by using fragility functions for bridge piers developed by Berry and Eberhard (Berry and Eberhard, 2003). The DMs considered for the rail were those corresponding to the damage states of train speed reduction (DMt1), track closure due to track misalignment (DMt2), and extensive track repair (DMt3), computed through the probabilistic model proposed by Pitilakis (Pitilakis et al, 2011). Median Column Drift Ratio ( $CDR_{0.5}$ ), Median Residual Drift Ratio ( $RDR_{0.5}$ ), and corresponding dispersion data for each DM fragility curve are provided in TABLE II.

TABLE II. DAMAGE MEASURES FRAGILITY CURVES PARAMETERS

Structure Damage Measures (DMs)			Track Damage Measures (DMt)		
DMs1: Yielding	$CDR_{0.5}=4.99 \cdot 10^{-3}$	$\sigma_{Ln}=0.30$	DMt1: Speed Reduction	$RDR_{0.5}=1.43 \cdot 10^{-3}$	$\sigma_{Ln}=0.7$
DMs2: Spalling	$CDR_{0.5}=2.87 \cdot 10^{-2}$	$\sigma_{Ln}=0.40$	DMt2: Track Closure	$RDR_{0.5}=5.74 \cdot 10^{-3}$	$\sigma_{Ln}=0.7$
DMs3: Buckling	$CDR_{0.5}=5.9 \cdot 10^{-2}$	$\sigma_{Ln}=0.26$	DMt3: Extensive Repair	$RDR_{0.5}=1.42 \cdot 10^{-2}$	$\sigma_{Ln}=0.7$

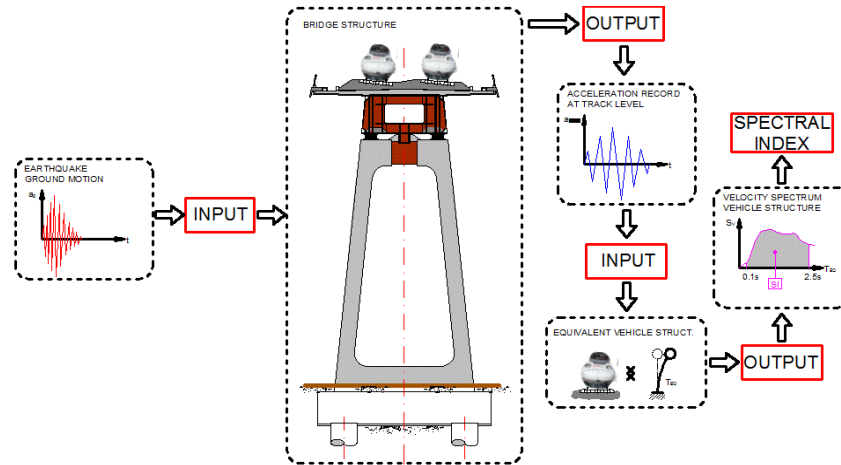


Figure 13. Spectral Index flow diagram for assessing derailment (Adapted from Luo and Miyamoto, 2007)

Furthermore, an assessment of the likelihood of train derailment was performed according to the methodology proposed by the Japanese Railway Administration (RTRI, 2007a). The Engineering Demand Parameter (EDP) considered for this assessment was the Spectral Index (Luo and Miyamoto, 2007). This index measures the vehicle likelihood of derailment (by both rocking and rolling derailment mechanisms) when subjected to transverse earthquake loading. It is computed as the integral of the velocity response spectrum of the vehicle motion (considered as a SDOF structure) between  $T_1=0.1s$  and  $T_2=2.5s$ , excited by a motion equal to the acceleration recorded or computed on top of the bridge (Figure 13).

The Spectral Index corresponding to derailment has been chosen as a sharp limit of  $SI=4100$  mm (161.4 in), which corresponds to the limit proposed for a Shinkansen vehicle type for this range of bridge oscillation periods (RTRI, 2007a). Although the dynamic characteristics of European trains are not equal to these of the Japanese lines, and due to the lack of data regarding this issue, this assumption can be seen as a first approach for the probabilistic analysis of derailment.

Response history analyses were carried out using a Newmark time integration algorithm ( $\beta=0.25$ ,  $\gamma=0.5$ ) assuming a constant acceleration between record sampling points. The convergence at each time step was achieved through a Newton-Raphson scheme, and a 5% Rayleigh damping pattern at 1<sup>st</sup> and 2<sup>nd</sup> modes of vibration was considered.

## SEISMIC PERFORMANCE

The seismic performance of the viaduct was evaluated by means of fragility curves relating the ground motion intensity (spectral acceleration at the characteristic period of each model) to the previously introduced damage measures (Collapse, derailment, structural DMs and track DMs). In what follows, we will interpretate the obtained fragility curves of each behavior model, in the light of the assumptions made for each of them.



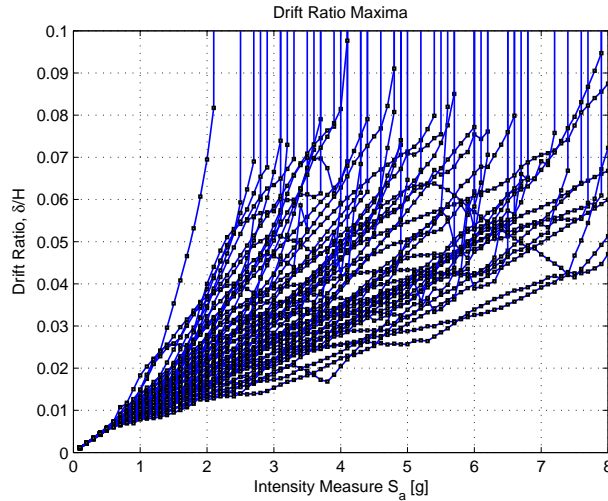


Figure 14. Incremental Dynamic Analysis with Maximum Drift Ratio as EDP.

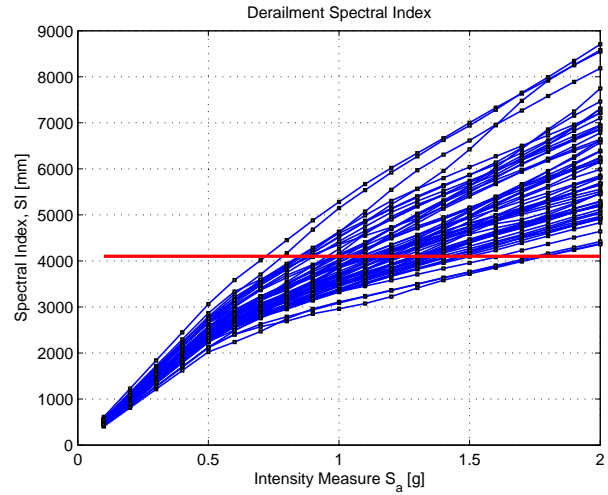


Figure 15. Incremental Dynamic Analysis with Spectral Index as EDP.

From the collapse fragility function (Figure 16), we can observe how for a given ground motion intensity, models on flexible foundation have a higher probability of collapse, and for a given foundation model, the probability of collapse under a given ground motion intensity increases as the period of vibration increases, since they undergo larger lateral deformations. However it should be noted that the probability of exceedance of a given spectral acceleration is not the same for all model and this probability in general decreases as the period of vibration increases.

For the derailment fragility function (Figure 17), we can observe how flexible structures exhibit considerably more risk of derailment than the stiffer structures. This is an intuitive result: given that the Spectral Index is related to the structure maximum pseudo-velocity, and therefore, a softer structural response that produces larger displacements and larger velocities increases dramatically the risk of derailment.

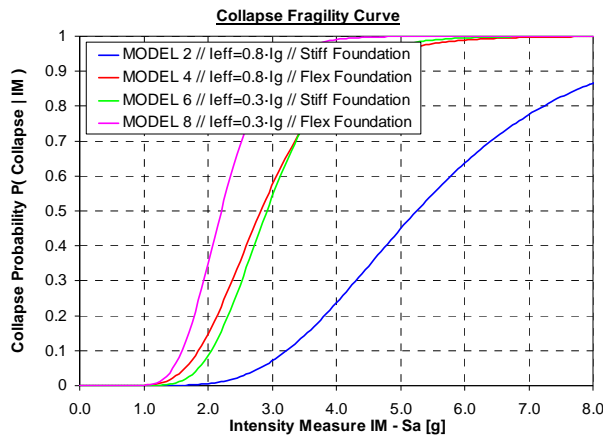


Figure 16. Collapse fragility curves for different behavior models

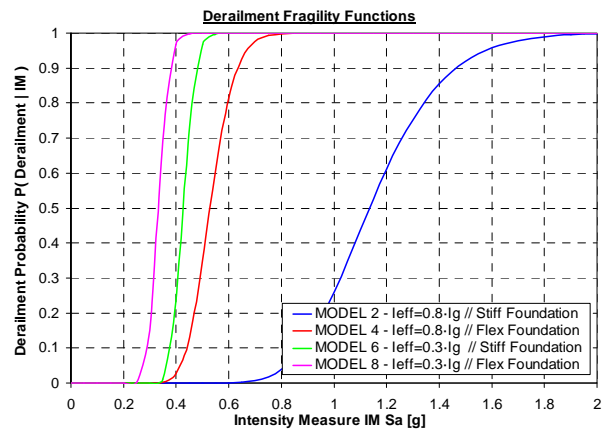


Figure 17. Derailment fragility curves for different behavior models

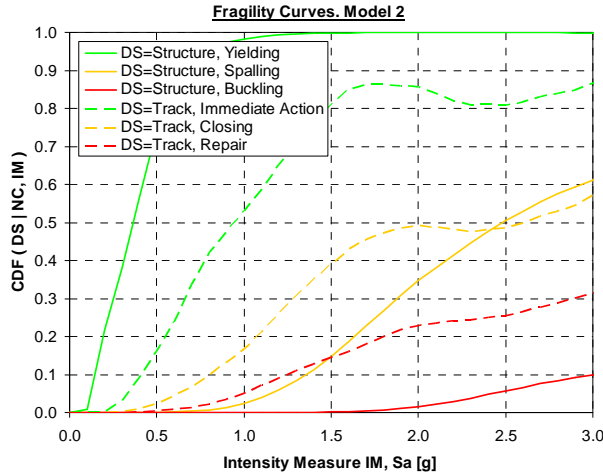


Figure 18. Structure and track fragility curves for model 2 ( $I_{\text{eff}}=0.8 \cdot I_g$ , Stiff foundation).

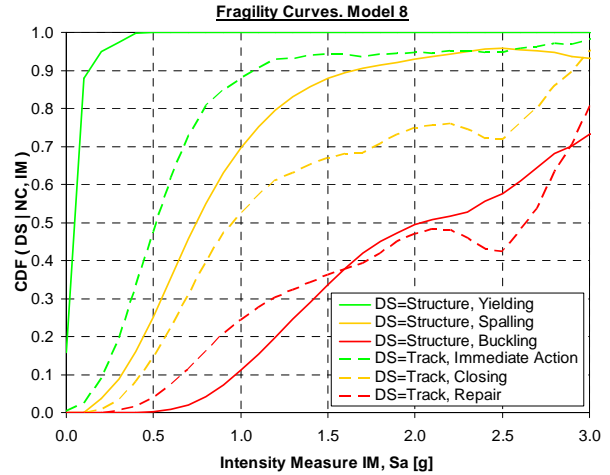


Figure 19. Structure and track fragility curves for model 8 ( $I_{\text{eff}}=0.3 \cdot I_g$ , Flexible foundation).

Regarding the fragility curves for the damage measures at the structure level and track level for different behavior models (Figure 18 and Figure 19), we can observe how, for the same intensity level, a softer response increases the risk associated to the track DMs. Given that the structure accommodates larger transient displacements by means of foundation rocking, the residual drift ratio larger than in the stiffer structure, yielding a larger track misalignment/offset at the end of the earthquake.

## CONCLUSIONS

A seismic performance assessment of a High-Speed Rail Line (HSRL) viaduct located in a region of moderate seismic hazard in the south of Spain has been performed. The performance assessment methodology developed by the Pacific Earthquake Engineering Research Center (PEER) has been extended to consider the performance of nonstructural components that are critical to the functionality of the HSRL.

The seismic response of a typical bent was carefully analyzed by conducting Incremental Dynamic Analyses in which the structure is subjected to ground motions scaled to increasing ground motion intensities. Record-to-record variability is explicitly considered in the analyses by using a relatively large number of ground motions (sixty) and computing the probability distribution of various response parameters at each level of ground motion intensity. Modeling uncertainty was considered by developing various detailed finite element models with different assumptions in both the piers and the foundation. Fragility functions were then used to estimate the probability of reaching different damage states for the structure and for the rail tracks.

In this paper, results have been summarized for four structural models resulting from combination of a flexible bent and a stiffer bent model on rigid and flexible foundations. All four models were found to have negligible probability of collapse for ground motions likely to occur at this site of moderate seismicity. Nevertheless, larger intensity levels were considered to study the relative performance of the various models. It is concluded that models that incorporate a flexible foundation experience larger lateral displacements relative to the ground than models on a rigid foundation and therefore lead to larger probabilities of collapse. Similarly, for a given

ground motion intensity and foundation model, the flexible bent models experience larger displacement demands than stiffer bent models leading to larger probability of collapse.

Damage measures for the rails indicate that probability of misalignments/offsets are significantly larger than probabilities of experiencing concrete cover spalling or buckling of longitudinal reinforcement, indicating that lateral deformations large enough to require rail repairs or realignment are smaller than those that would lead to significant structural damage. In particular, the probability of experiencing residual deformations increases significantly once ground motion intensities leading to yielding of the structure are reached.

The approach used here for the evaluation of this viaduct provides a rational framework that explicitly considers uncertainties in the ground motion intensity, the structural response, the damage as well as the consequences of the damage on the functionality of the high-speed rail.

## REFERENCES

- Aviram, A. Mackie, K. R. Stojadinovic, B. (2008) "Guidelines for Nonlinear Analysis of Bridge Structures in California". *Pacific Earthquake Engineering Research Center Report*; UCB/PEER 2008/03.
- Benito, M. B. Navarro, M. Vidal, F. Gaspar-Escribano, J. Garcia-Rodriguez, M. J. Martinez-Solares, J. M. (2010) "A new seismic Hazard assessment in the region of Andalusia (Southern Spain)". *Bulletin of Earthquake Engineering*, Vol. 8, pp. 739-766.
- Berry, M. Eberhard, M. (2003) "Performance Models for Flexural Damage in Reinforced Concrete Columns". *Pacific Earthquake Engineering Research Center Report*; UCB/PEER 2003/18.
- EN-1991-2 (2003). "Eurocode 1: Actions on structures – Part 2: Traffic loads on bridges". European Committee for Standardization, Brussels.
- EN-1992-1 (2004). "Eurocode 2: Design of concrete structures – Part 1-1: Traffic General rules and rules for buildings". European Committee for Standardization, Brussels.
- EN-1998-1 (2004). "Eurocode 8: Design of structures for earthquake resistance – Part 1: General rules, seismic actions and rules for buildings". European Committee for Standardization, Brussels.
- EN-1998-2 (2005). "Eurocode 8: Design of structures for earthquake resistance – Part 2: Bridges". European Committee for Standardization, Brussels.
- Fardis, M. N. Biskinis, D. (2003) "Deformation Capacity of RC Members, as Controlled by Flexure or Shear". *Proceedings of the Otani Symposium*; pp. 511-530.
- Fardis, M. N. (2009) "Seismic Design, Assessment and Retrofitting of Concrete Buildings - Based on EN-Eurocode 8". Springer-Verlag, New York.
- Hasselton, C. Deierlein, G. (2007) "Assessing Seismic Collapse Safety of Modern Reinforced Concrete Moment Frame Buildings". *John A. Blume Engineering Center Report*; No. 156.
- Hess, J. (2009) "Rail Expansion Joints - The Underestimated Track Work Material?". *Track-Bridge Interaction on High Speed Railways*. pp. 149-164. Taylor & Francis, London.
- Ibarra, L. F. Medina, R. A. Krawinkler, H. (2005) "Hysteretic Models that Incorporate Strength and Stiffness Deterioration". *Earthquake Engineering & Structural Dynamics*; Vol. 34, pp. 1489-1511.
- Jeremic, B. Kunnath, S. Xiong, F. (2004) "Influence of soil–foundation–structure interaction on seismic response of the I-880 viaduct". *Engineering Structures*; Vol. 26, No. 3, pp. 391-402.
- Krawinkler, H. Miranda, E. (2004) "Chapter 9 – Performance Based earthquake Engineering". *Earthquake Engineering*, Bozorgnia, Y. Bertero, V. V. Eds. CRC Press.
- Kunnath, S. K. Larson, L. Miranda, E. (2006) "Modelling considerations in probabilistic performance-based seismic evaluation: case study of the I-880 viaduct". *Earthquake Engineering & Structural Dynamics*; Vol. 35, pp.57-75.
- Kunnath, S. K. (2007) "Application of the PEER PBEE Methodology to the I-880 Viaduct". *Pacific Earthquake Engineering Research Center Report*; UCB/PEER 2006/10.
- Luo, X. (2005) "Study on methodology for running safety assessment of trains in seismic design of railway structures". *Soil Dynamics and Earthquake Engineering*; Vol. 25, No. 2, pp. 79-91.
- Luo, X. Miyamoto, T. (2007) "Method for Running Safety Assessment of Railway Vehicles against Structural Vibration Displacement during Earthquakes". *Quarterly Report of RTRI*; Vol. 48, No. 3, pp. 129-135.

- Mackie, K. R. Stojadinovic, B. (2004) "Fragility Curves for Reinforced Concrete Highway Overpass Bridges". *Proceedings of the 13 th World Conference on Earthquake Engineering*; No. 1553, pp. 1-14.
- Mander, John B, Priestley, Michael J. N. Park, R. (1988) "Theoretical stress-strain model for confined concrete". *Journal of Structural Engineering*; Vol. 114, No. 8, pp. 1804-1826.
- Mander, J. B. Dhakal, R. P. Mashiko, N. Solberg, K. (2007) "Incremental Dynamic Analysis applied to Seismic Financial Risk Assessment of Bridges". *Engineering Structures*; Vol. 29 No. 10, pp. 2662-2672.
- Millanes-Mato, F. Matute-Rubio, L. Ortega-Cornejo, M. Martinez-Agromayor, D. Bordo-Bujalance, E. (2011) "Development of Steel and Composite solutions for viaducts on Spanish High-Speed Railway Lines" (in Spanish). *Hormigon y Acero*; Vol. 62, No. 259, pp. 7-27.
- Millanes-Mato, F. Bordo-Bujalance, E. Martin-Suarez, J. Mansilla-Dominguez, J. L. (2011) "The Archidona Viaduct (HSRL Cordoba-Granada). A 3,150 m long steel-concrete composite deck without intermediate expansion joints" (in Spanish). *Comunicaciones al V Congreso de ACHE*; pp. 1-11.
- Mosher, R. L. Dawkins, W. P. (2000) "Theoretical Manual for Pile Foundations". US Army Corps of Engineers. Engineer Research and Development Center.
- Nasarre, J. (2009) "Serviceability limit states in relation to the track in railway bridges". *Bridges for High Speed Railways*. pp. 211-220. Taylor & Francis, London.
- NCSP-07 "Spanish Earthquake Resistant Code: Bridges" (in Spanish). Ministerio de Fomento, Madrid.
- Nishimura, A. (2004) Damage Analysis and Seismic Design of Railway Structures for Hyogoken-Nanbu (Kobe) Earthquake. *Journal of Japan Association for Earthquake Engineering*; Vol. 4, No. 3, pp. 184-194.
- OpenSees. Open system for earthquake engineering simulation. 2004, <http://opensees.berkeley.edu>.
- PEER Ground Motion Database. [http://peer.berkeley.edu/peer\\_ground\\_motion\\_database/](http://peer.berkeley.edu/peer_ground_motion_database/).
- Pitilakis, K. Argyroudis, S. Kaynia, A. M. Johansson, J. (2011) "Fragility Functions for Railway System Elements". *Systemic Seismic Vulnerability and Risk Analysis for Buildings, Lifeline Networks and Infrastructures Safety Gain*, D 3.8, Syner-G Report; May 31, 2011.
- PoLam, I. Kapushar, M. Chaudhuri, D. (1998) "Modeling of Pile Footings and Drilled shafts for Seismic Design". Technical Report MCEER-98-0018. Multidisciplinary Center for Earthquake Engineering Research, Buffalo.
- Priestley, M. J. N. Seible, F. Calvi, G. M. (1996) "Seismic Design and Retrofit of Bridges". John Wiley & Sons, New York, NY.
- Railway Technical Research Institute, ed (2007a) "Design Standards for railway Structures and Commentary (Displacement Limits)". Railway Bureau of the Ministry of Land, Infrastructure and Transport, Tokyo.
- Railway Technical Research Institute. ed (2007b) "Design Standards for railway Structures and Commentary (Seismic Design)". Railway Bureau of the Ministry of Land, Infrastructure and Transport, Tokyo.
- Sugano, S. ed. (2007) "Seismic Rehabilitation of Concrete Structures". American Concrete Institute and Japan Concrete Institute. Farmington Hills, MI.
- Terzic, V. Stojadinovic, B. (2010) "Post-Earthquake Traffic Capacity of Modern Bridges in California". *Pacific Earthquake Engineering Research Center Report*; UCB/PEER 2010/103.
- Vamvatsikos, D. Cornell, C. A. (2002) "Incremental Dynamic Analysis". *Earthquake Engineering & Structural Dynamics*; Vol. 31, pp. 491-514.
- Yoshikawa, H. Ohtaki, T. Hattori, H. Maeda, Y. Noguchi, A. Okada, H. (2007) "Seismic risk assessment and expected damage evaluation of railway viaduct". *Applications of Statistics and Probability in Civil Engineering*. Taylor & Francis Group, London.